Available online at www.sciencedirect.com
SCIENCE DIRECT
Brain Research 1035 (2005) 1–12
BRAIN RESEARCH
www.elsevier.com/locate/brainres

Research report

Neuroanatomical distribution of vasotocin and mesotocin in two urodele amphibians (*Plethodon shermani* and *Taricha granulosa*) based on in situ hybridization histochemistry

David M. Hollis[a], Joanne Chu[b], Eliza A. Walthers[c], Bethany L. Heppner[c], Brian T. Searcy[c], Frank L. Moore[c,*]

[a]*Great Lakes WATER Institute, University of Wisconsin-Milwaukee, Milwaukee, WI 53204, USA*
[b]*Department of Biology, Spelman College, Atlanta, GA 30314, USA*
[c]*Department of Zoology, Oregon State University, Corvallis, OR 97331, USA*

Accepted 16 November 2004
Available online 25 January 2005

Abstract

Previous research suggests that considerable species-specific variation exists in the neuroanatomical distributions of arginine vasotocin (AVT) and mesotocin (MST), non-mammalian homologues of vasopressin and oxytocin. An earlier study in rough-skinned newts (*Taricha granulosa*) indicated that the neuroanatomical distribution of cells labeled for AVT-immunoreactivity (ir) was greater in this urodele amphibian than in any other species. It was unknown whether the widespread distribution of AVT-ir is unique to *T. granulosa* or a feature common among salamanders. Using in situ hybridization (ISH) histochemistry and gene-specific riboprobes, the current study labeled AVT and MST mRNA in *T. granulosa* and the red-legged salamander (*Plethodon shermani*). In *T. granulosa*, AVT ISH-labeled cells were found to be widespread and localized in brain areas including the dorsal and medial pallium, lateral and medial septum, bed nucleus of the stria terminalis, amygdala, preoptic area, ventral hypothalamus, nucleus isthmus, tectum mesencephali, inferior colliculus, and hindbrain. In *P. shermani*, the distribution of AVT ISH-labeled neurons matched that of *T. granulosa*, except in the lateral septum, ventral hypothalamus, and inferior colliculus, but did however include labeled cell bodies in the lateral pallium. The distribution of MST ISH-labeled cells was more restricted than AVT ISH labeling and was limited to regions of the preoptic area and ventral thalamus, which is consistent with the limited distribution of MST/OXY in other vertebrates. These findings support the conclusion that urodele amphibians possess a well-developed vasotocin system, perhaps more extensive than other vertebrate taxa.

Theme: Neurotransmitters, modulators, transporters, receptors
Topic: Peptides: anatomy and physiology

Keywords: Amphibian; Vasotocin; Mesotocin; Vasopressin; Oxytocin

1. Introduction

Arginine vasotocin (AVT) and mesotocin (MST) are structurally similar nonapeptides, differing from each other by only two amino acid residues and both belonging to the neurohypophysial peptide family. AVT has been found in many species of non-mammalian vertebrates from cyclostomes to birds [2,4,20,39,45,53,54], and is the ancestral orthologous peptide of arginine vasopressin (AVP) found in mammals [3]. MST has been found in lung-fishes, amphibians, reptiles, birds, and marsupials, and is the ancestral peptide for oxytocin (OXY) in eutherian mammalians [4].

Neurohypophysial peptides were first identified as hormones secreted from nerve terminals in the pars

* Corresponding author. Fax: +541 737 0501.
E-mail address: mooref@science.oregonstate.edu (F.L. Moore).

0006-8993/$ - see front matter © 2005 Elsevier B.V. All rights reserved.
doi:10.1016/j.brainres.2004.11.051

nervosa and as having a variety of endocrine functions. AVT and AVP regulate hydromineral balance, vascular tone, and glucose metabolism; whereas, OXY controls smooth muscle contractions associated with parturition, lactation, and sexual arousal [1,22,41]. Less is known about the endocrine functions of MST; although MST has been shown to play a role in parturition in a marsupial mammal [10]. Neurohypophysial peptides also act centrally as neurotransmitters and neuromodulators, and appear to regulate a wide variety of brain functions and behaviors [7,26,40,50,58].

Consistent with the diverse central and peripheral functions attributed to neurohypophysial peptides, neuroanatomical studies reveal complex and, perhaps, species-specific neuroanatomical patterns of distribution. Immunocytochemical (ICC) and/or in situ hybridization (ISH) studies have found that, in most non-mammalian species, cell bodies labeled for AVT and MST are localized in the anterior hypothalamus/preoptic areas that are homologous to the AVP- and OXY-containing cell bodies in the paraventricular and supraoptic nuclei of mammals [12,15,19,28,29,49,51,60,63,64]. In addition to these conserved populations of cells, neurohypophysial peptide-containing cells reportedly occur in a variety of other sites in the brain [26,30,51,57]. But it is unknown whether these variations in neurohypophysial distribution within the brain reflect differences in techniques, species differences, sexual dimorphism, or other factors.

A previous ICC study from our laboratory identified at least nineteen distinct populations of AVT-immunoreactive (ir) cells in brains of rough-skinned newts (*Taricha granulosa*) [46,51], which suggested that this amphibian might have a more widespread distribution of AVT-ir cells than other species [46,51]. Thus the questions addressed by the current study are (1) whether the same nineteen populations of AVT-ir neurons can be identified using ISH techniques to label AVT mRNA and (2) whether the widespread distribution of AVT in *T. granulosa* is unique to this species or occurs in another species of salamander, the red-legged salamander (*Plethodon shermani*). To answer these two questions and also to identify the neuroanatomical distribution of MST in both species of salamanders, the current study used ISH techniques and species-specific riboprobes. Prior neuroanatomical studies for AVT and MST in amphibians have been limited to using ICC techniques with heterologous antibodies, mainly antisera generated against mammalian AVP or OXY [6,17,23–25,36,42,46]. To our knowledge, the only ISH study of AVT and MST systems in an amphibian was our work with *T. granulosa* [46], and that study used ISH with heterologous oligonucleotide probes. That earlier ISH study was not sensitive and, mainly, was used to validate the ICC procedures. The current study reports for the first time the neuroanatomical distribution of AVT and MST ISH-labeled cells using species-specific cRNA probes in the brain of amphibians.

2. Materials and methods

2.1. Animal collection and care

Conditions of captivity for each species differed to reflect particular aspects of their respective natural environments. Adult *P. shermani* were collected in forests and near streams in Macon County, NC, during the breeding season in August, and were maintained in an environmentally-controlled room (12.7 °C, 70% humidity, 12:12 LD cycle), housed individually in plastic boxes (30.5 cm length, 15.2 cm width, 8.9 cm depth) containing moist paper towels and moss, and fed mealworms. Adult *T. granulosa* were collected from local ponds in Lincoln County, OR, during the breeding season in March and April or out of the breeding season in November, and were maintained in an environmentally-controlled room (7 °C; 12:12 LD cycle) and housed together in a large, cylindrical tank (91 cm diameter, 78 cm height) with flow-through dechlorinated water (depth about 39 cm), and fed bloodworms and earthworms.

Salamanders were anesthetized by chilling and then rapidly decapitated. The brain and rostral spinal cord were rapidly dissected (1–2 min) and embedded in Histoprep Frozen Tissue Embedding Media (Fisher Scientific, Pittsburgh, PA), frozen on dry ice, and stored at −80 °C until sectioning. Whole brains were sectioned at a thickness of 20 μm at −20 °C using a Cryostat. The sections were thaw-mounted on Superfrost Plus® positive-charged microscope slides (Shandon, Inc., Pittsburgh, PA) and stored at −80 °C until use.

Neuroanatomical analysis with *T. granulosa* used a total of 20 brains from sexually mature males (15 males in breeding condition and 5 males not in breeding condition). All *T. granulosa* were held in captivity for less than a week.

Neuroanatomical studies with *P. shermani* used a total of 30 brains collected from sexually mature males ($n = 10$) or females ($n = 20$). Female *P. shermani* were sacrificed during the breeding season, within 8 weeks of capture; whereas male *P. shermani* were sacrificed after the breeding season when secondary sexual traits were regressed [37] and after about 16 weeks in captivity. Our main objective was to identify the neuroanatomical distribution of neurons that synthesize AVT or MST by using species-specific riboprobes and ISH procedures. This study was not designed to reveal differences in AVT and MST expression in males versus females, or breeding versus non-breeding animals, in part because the ICC study with *T. granulosa* has already reported sexual and seasonal differences in AVT immunoreactivity [52].

This study was performed under the guidelines of the U.S. Public Health Service's "Guide to the Care and Use of Laboratory Animals". All procedures were approved by the Oregon State University Laboratory Animal Resource Committee.

2.2. cRNA probe synthesis

The cDNA sequences that encode the AVT and MST preprohormones in *P. shermani* or *T. granulosa* were determined using RT-PCR and 5′ and 3′ RACE PCR protocols. Based on nucleotide sequences for AVT and MST from each salamander, gene-specific primers were designed to amplify cDNA fragments to be used as templates for making gene-specific cRNA probes (riboprobes), with the exception of the degenerate primers used in the initial isolation of the *P. shermani* MST preprohormone. The primers used were, for *T. granulosa* AVT (forward; 5′-GAGGCGGCAAGAGGTCTTT-3′, reverse; 5′-GGTGCAGCTCACGTCACTAC-3′), for *T. granulosa* MST (forward; 5′-TTGTCTTCAGCCTGCTACATCC-3′, reverse; 5′-CAGCCGGTCTAGGAAAACG-3′), for the *P. shermani* AVT (forward; 5′-AGGAGGCAAGCGCTCCTT-3′, reverse; 5′-GGTGCAGCTCTCATCACTGC-3′), and for the *P. shermani* MST (forward; 5′-AAYTGYCC-CATHGGMGGXAARMG-3′, reverse; 5′-GGSAGRWART-TYTCYTCCT GGCAVCT-3′). The cDNA fragments were ligated into pCR TOPO 4 and amplified in *E. coli* using the TOPO TA Cloning® Kit for Sequencing (Invitrogen™, San Diego, CA). Following the methods of Maniatis [47] and Birnboim and Doly [14], large-scale plasmid-preps were performed by alkaline lysis. The plasmids containing the appropriate cDNA insert were then linearized with either *Spe*I or *Not*I restriction enzymes. The linearized plasmid was used as a template in an in vitro transcription reaction to produce the cRNA probe using the RNA polymerase T7 or T3 to yield sense and anti-sense probes, respectively. In vitro transcription was performed in the presence of 500 μM each of ATP, CTP, and GTP, and 6 μM UTP, and 6 μM [^{35}S]-UTP (specific activity = 1200 Ci/mmol; ICN, Aurora, OH). Finally, the probes were purified by phenol/chloroform (1:1, pH 5.2) extraction and two ethanol precipitations in the presence of 0.4 M sodium chloride, and re-suspended in 50 μl 0.1% sodium dodecyl sulfate (SDS). The probes were stored at −80 °C until use.

The *P. shermani* and *T. granulosa* AVT preprohormone cRNA probes were 252 and 254 bases, respectively. The MST preprohormone probes for *P. shermani* and *T. granulosa* were 186 and 236 bases, respectively.

2.3. In situ hybridization

The in situ hybridization technique followed the methods of Zoeller et al. [70], with modifications as described. Mounted tissue slices were prepared for fixation and prehybridization washes by thawing frozen sections on glass slides at room temperature. The tissue slices were fixed for 30 min (4% paraformaldehyde) in 1× phosphate-buffered saline (PBS; 0.15 M NaCl, 1.0 mM KH_2PO_4, 6.0 mM Na_2HPO_4) and then rinsed twice in 1× PBS for 2 min. Acetylation then occurred by immersing the tissue in 0.45% sodium chloride containing 0.1 M triethanolamine-hydrochloride (pH 8.0), and 0.25% acetic anhydride (added just before use) for 10 min. After a 2-min rinse in 1× standard saline citrate (SSC; 0.15 M NaCl, 0.015 M Na_3Citrate), tissue was dehydrated through a series of increased concentrations of ethanol (70% ethanol for 1 min, 80% ethanol for 1 min, 95% ethanol for 2 min, and 100% ethanol for 1 min) and delipidated in chloroform (5 min). Finally, tissue was partially rehydrated by sequential immersion in 100% ethanol (2 min) and 95% ethanol (2 min). Tissue was dried for 30 min and then covered in hybridization solution, which contained 50% deionized formamide, 0.1% sodium pyrophosphate, 10% dextran sulfate, 2× SSC, 25 μg/ml tRNA, 200 mM dithiothreitol, and 1× Denhardt's solution (0.02% each of bovine serum albumin, Ficoll, and polyvinylpyrrolidone), and the appropriate volume of [^{35}S]-UTP-labeled cRNA probe (2,000,000 cpm/slide). Finally, parafilm coverslips were placed over the hybridization solution and the slides were placed on a rack in an air-tight plastic box containing 50 ml of water to provide a humid environment while in an incubator for 20 h at 52 °C.

After incubation, parafilm coverslips were removed by dipping the slides in 1× SSC. Slides were then washed four times for 15 min in 1× SSC, placed in two 20-min washes of 2× SSC/50% deionized formamide at 52 °C, and then rinsed twice for 10 min in 2× SSC at room temperature. Tissue was incubated in RNase wash buffer (0.5 M sodium chloride, 0.01 M Tris, 1 mM EDTA; pH 8.0) at 37 °C for 10 min, followed by 30 min incubation in RNase A (Sigma, St. Louis, MO; 100 μg/ml in RNase wash buffer) at 37 °C. The tissue was then rinsed twice in 2× SSC for 10 min and placed in two additional 20-min washes of 2× SSC/50% deionized formamide at 52 °C and two rinses for 10 min in 1× SSC at room temperature. Finally, slides were placed in 70% ethanol twice for 5 min and then allowed to dry for at least 30 min. After drying, slides were individually dipped in Kodak NTB-2 emulsion film (Rochester, NY) at 42 °C, dried for 3 h at room temperature, and allowed to expose for 28 days at 4 °C. Following exposure, slides were developed in Dektol developer (Kodak, or VWR Rochester NY) for 2 min, placed in a stop bath (deionized, distilled H_2O) for 30 s, and fixed in full strength fixer (Kodak, Rochester, NY) for 5 min (all chemicals used in the development were maintained at between 12 and 14 °C). Slides were then washed in running tap water for 5 min. Afterward, tissue was counterstained with 0.1% methyl green for 30 s, followed by a 2–3 min wash in running tap water, and finally dehydrated in 50% ethanol for 30 s. Slides were dried for at least 15 min, cover-slipped using Permount Histological Mounting Medium (Fisher Scientific, Santa Clara, CA), and analyzed with light microscopy.

2.4. Nomenclature

Nomenclature for specific brain loci is italicized if it comes from the work of Herrick [33,34] or is printed in

normal fonts if the nomenclature comes from Northcutt and Kicliter [55].

3. Results

3.1. Validation of ISH technique

In control ISH studies that used species-specific cRNA probes with nucleotide sequences matching the sense strand of AVT or MST, no specifically labeled cells were found in *T. granulosa* or *P. shermani*. In contrast, the ISH protocol in this study labeled specific cells using species-specific cRNA probes with nucleotide sequences matching anti-sense strands of AVT or MST.

3.2. Neuroanatomical distribution of AVT ISH-labeled cells in P. shermani and T. granulosa

The overall pattern of ISH labeling with AVT cRNA was widespread in both species of salamander in general, but with a few notable exceptions, and corresponded with the neuroanatomical distribution of the AVT system described earlier by ICC in *T. granulosa* [46]. Thus, salamanders appear to have a more extensively developed AVT system than other vertebrate taxa.

In the previous ICC study [46], Lowry et al. identified nineteen distinct populations of AVT-ir cells based on similarities in cytoarchitecture and anatomical location. These AVT-ir cell populations are often not confined within the boundaries of specific brain nuclei or anatomical landmarks, which makes them difficult to describe with simple anatomical labels. Therefore, to assist with communication, the current paper uses Lowry's system of labeling AVT populations as V1 through V19 to complement descriptions of the anatomical locations of AVT ISH-labeled cells.

In the telencephalon of both species, AVT ISH-labeled cells were observed in the *primordium pallii dorsalis* (V1), also referred to as the dorsal pallium. Both species had AVT ISH-labeled cells localized in the dorsal pallium just dorsal to the medial pallium. AVT ISH-labeled cells were most common in the dorsal aspects of the dorsal pallium, especially in *T. granulosa*. Labeled cells in the dorsal pallium were commonly found in *T. granulosa* to extend from rostral regions to the mid-telencephalon, with labeled cells rarely in the caudal poles. In *P. shermani*, AVT ISH-labeled cells in the dorsal pallium were not observed in every individual and, when found, were more variable and not as localized to the dorsal aspects of the dorsal pallium. Also in *P. shermani*, although some individuals had AVT ISH-labeled cells in mid-telencephalic regions of the dorsal pallium, others only had labeled cells in the caudal poles of the telencephalon, at the level of the optic chiasma.

In the *primordial hippocampi* (V2), referred to as the medial pallium, the AVT ISH-labeled cells were found to extend from the extreme rostral end of the medial pallium, just caudal to the *nucleus olfactorius anterior pars medialis*, to its extreme posterior, in the caudal poles of the telencephalon (Figs. 1A and 2A), often as caudal as the level of the *commissura habenularum*. The pattern of labeled cells was similar in both species. Numbers of AVT ISH-labeled cells in the medial pallium on one side of a frontal section varied from as low as two to three cells to 30–40 cells. Typically, the numbers of AVT ISH-labeled cells increased in the caudal aspects of the medial pallium and were greatest at levels also containing the amygdala and preoptic area. At this level, AVT ISH-labeled cells in the medial pallium also extended ventrally into the *commissura hippocampi* and medially into the *pars fimbrali septi*. Numbers of AVT ISH-labeled cells were fewer in the caudal aspect of the medial pallium. AVT ISH labeling in individual cells of the medial pallium was often very dense and appeared particularly distinct.

In *P. shermani*, AVT ISH-labeled cells occurred in the *nucleus olfactorius dorsolateralis* (lateral pallium), just dorsal to the lateral cellular prominence. In *T. granulosa*, no AVT ISH-labeled cells were found in the lateral pallium, which is consistent with our earlier ICC study; thus these AVT cells were not identified previously. In *P. shermani*, the AVT ISH-labeled cells in the lateral pallium were also found just dorsal of the lateral cellular prominence. Interestingly, the most common occurrence of AVT ISH labeling in the lateral pallium in *P. shermani* was a single, individual cell (per one side of a frontal section) bordering the lateral ventricle just ventral to the dorsal pallium. AVT ISH-labeled cells also occurred in the lateral pallium in the caudal poles of the telencephalon (typically one per side on a frontal section), at the level where both the optic chiasma and ventral habenular nucleus were present [34].

In both species, AVT ISH-labeled cells were found in the *nucleus medialis septi*, or medial septum (V3). At the level of the mid-telencephalon, this labeling typically included only one or two cells on each side of a frontal section. However, in the caudal telencephalon, at the level where the *nucleus lateralis septi* (lateral septum) is absent [34], AVT ISH-labeled cells in the medial septum persisted into the *pars fimbrali septi*, often in a single row of two to four cells on each side of a frontal section. These cells were typically more intensely labeled than cells in the rostral aspects of the medial septum.

In *T. granulosa*, but not *P. shermani*, AVT ISH-labeled cells were found in the ventromedial region of the telencephalon within the lateral septum. These AVT ISH-labeled cells extended into the ventrolateral region of the medial pallium, but were easily distinguished as part of the lateral septum by their location ventral to the *sulcus limitans hippocampi* and dorsal to the *sulcus limitans septi* [34]. Typically, this labeling was restricted to a single, densely labeled cell on both sides of a frontal section per individual and appears to represent a previously unidentified population of AVT-producing cells.

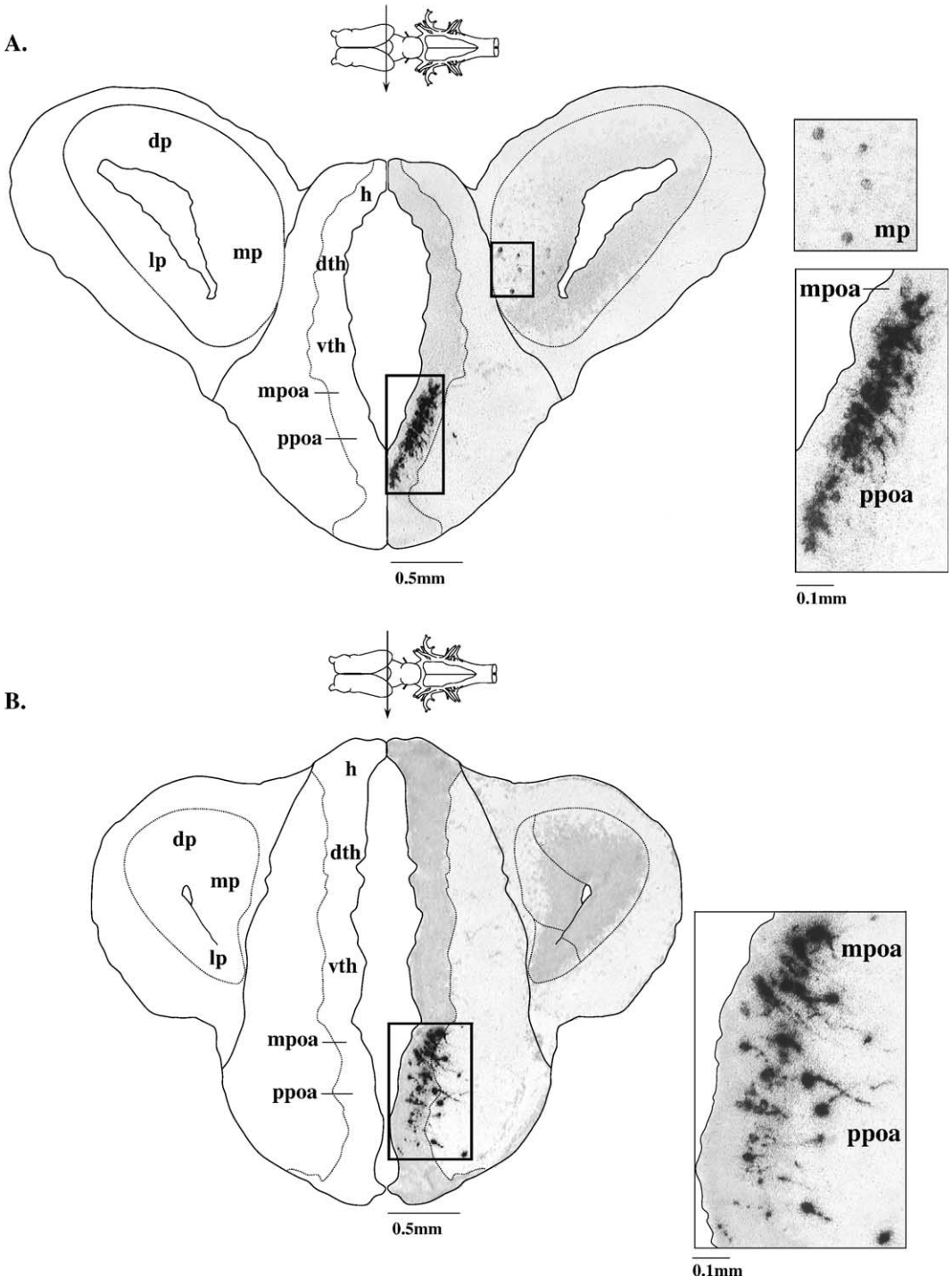

Fig. 1. Neuropeptide ISH labeling in the brain of *T. granulosa*. (A) Photomicrograph (right) of AVT ISH labeling in the medial pallium, magnocellular preoptic area, and posterior preoptic area at the level of the habenular nuclei in the frontal section (magnification = 40×). Major neuroanatomical areas are indicated on the left. Boxes show ISH labeling at higher magnification (200×). (B) MST ISH labeling in the magnocellular and posterior preoptic areas at a level just caudal to the frontal section shown above in A. h, habenula; dp, dorsal pallium; dth, dorsal thalamus; lp, lateral pallium; mp, medial pallium; mpoa, magnocellular preoptic area; ppoa, posterior preoptic area; vth, ventral thalamus.

In the caudal telencephalon of both species, AVT ISH-labeled cells were observed in the *prominentia ventralis* (bed nucleus of the stria terminalis) (V4). Typically, this population consisted of a small cluster of cells per frontal section in *T. granulosa* and only one or two labeled cells per frontal section in *P. shermani*.

Both species had AVT ISH-labeled cells in the *nucleus amygdalae dorsolateralis* and *nucleus amygdalae* (V5). These AVT-labeled cells typically consisted of two or three positive cells in dorsal aspect of the amygdala dorsolateralis, localized near the ventral border of the lateral pallium and just ventral to the lateral cellular prominence. In some

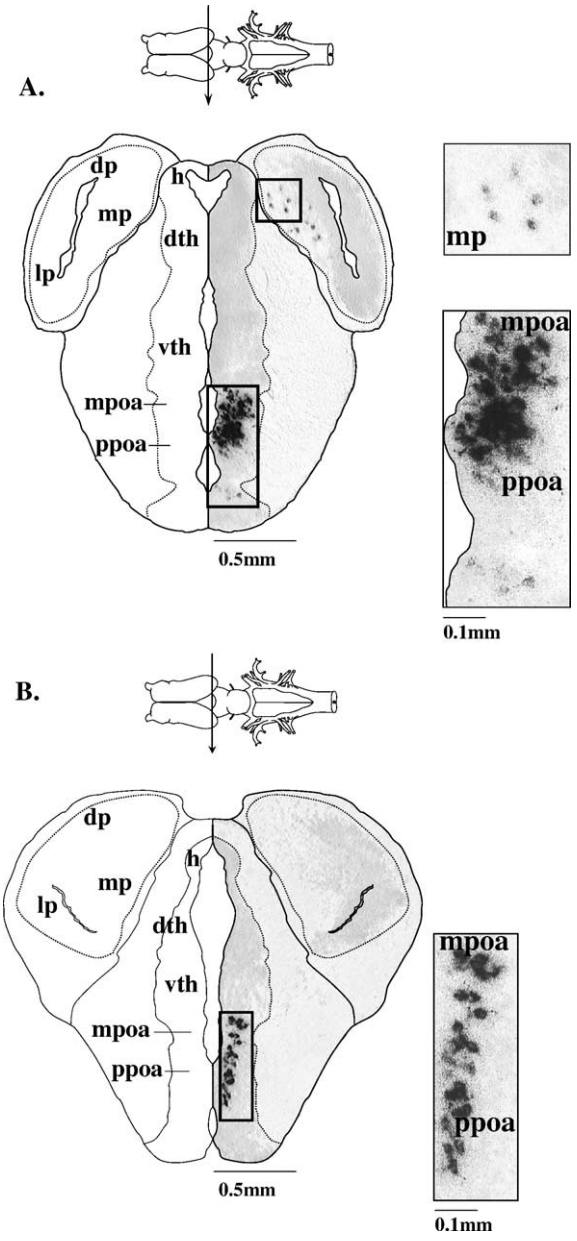

Fig. 2. Neuropeptide ISH labeling in the brain of *P. shermani*. (A) Photomicrograph (right) of AVT ISH labeling in the medial pallium, magnocellular preoptic area, and posterior preoptic area at the level of the habenular nuclei in the frontal section (magnification = 40×). Major neuroanatomical areas are indicated on the left. Boxes show ISH labeling at higher magnification (200×). (B) MST ISH labeling in the magnocellular and posterior preoptic areas at a level slightly rostral to the frontal section shown above in A. See Fig. 1 for abbreviations.

individuals from both species, however, AVT ISH-labeled cells occurred in a more ventral and caudal location within the *nucleus amygdalae dorsolateralis*, at the level of the rostralmost *nucleus preopticus pars anterior* (anterior preoptic area). AVT ISH-labeled cells were also concentrated in an area medial to the *nucleus amygdalae dorsolateralis* and lateral to the *bed nucleus of the decussation of the fasciculus laterals telencephali*, namely the *nucleus amygdalae*. In *P. shermani*, but not *T. granulosa*, some individuals contained a continuum of AVT ISH-labeled cells that extended from the ventral aspect of the *nucleus amygdalae dorsolateralis* into the *nucleus amygdalae*.

In both species, the AVT ISH-labeled cells were found in the *bed nucleus of the decussation of the fasciculus lateralis telencephali* (V6), which is located dorsal to the bed nucleus of the stria terminalis, medial to the *nucleus amygdalae*, and rostral to the level of the *eminentia thalami* (thalamic eminence) [34]. Typically, only one or two labeled cells per frontal section were found at this site.

Compared to other brain regions, AVT ISH-labeled cells were most abundant and most intensely labeled in the preoptic area. In the *nucleus preopticus pars anterior* (anterior preoptic area) (V7), AVT ISH-labeled cells extended both rostrocaudally and dorsoventrally. Typically, AVT mRNA containing cells of the anterior preoptic area extended rostrocaudally from the level of the rostralmost portion of the thalamic eminence (just caudal to the *pars fimbrialis septi*), to the most rostral aspect of the *pars ventralis thalami* (ventral thalamus, V8; discussed below) [34]. At this level, the anterior preoptic area lies ventral to the *nucleus preopticus pars posterior* (posterior preoptic area) [34] and is often referred to as the ventral preoptic area (V11), which had AVT ISH-labeled cells that were indistinguishable from labeled cells in the posterior preoptic area.

In the posterior preoptic area (V10), AVT ISH-labeled cells were extremely dense and broadly distributed, extending the entire length of the region dorsoventrally (see Fig. 1A). Although these AVT mRNA labeled cells were typically located medially along the *recessus preopticus* in both species, they also extended laterally as well (see Fig. 2A). At the level of the rostral *nucleus ventralis habenulae* (ventral habenular nucleus), AVT ISH-labeled cells in the posterior preoptic area extended both ventrally into the anterior (ventral) preoptic area (V11) and dorsally into, and throughout, the *pars magnocellularis of the preoptic nucleus* [35], the magnocellular preoptic area (V9) (Figs. 1A and 2A). At the level of the rostralmost *nucleus dorsalis habenulae* (dorsal habenular nucleus), AVT ISH-labeled cells were markedly reduced in number in the posterior preoptic area, but a few densely labeled cells persisted dorsolaterally in the magnocellular preoptic area.

Both species had AVT ISH-labeled cells in the caudalmost portion of the magnocellular preoptic area, at the level just rostral to the *commissura postoptica*, and extending into the ventralmost region of the ventral thalamus (V8). In some individuals of both species, AVT ISH labeling was observed in cells in the central region of the ventral thalamus at the level just rostral to the ventral habenular nucleus.

In contrast to the earlier ICC study, AVT ISH-labeled cells were not found in the *pars dorsalis hypothalami* (dorsal hypothalamus) (V12) or *primordial mammillary region* (lateral region of the dorsal hypothalamus) (V14) in either species. In *T. granulosa*, but not *P. shermani*, AVT ISH labeling occurred in *the posterior lobe of the pars*

ventralis hypothalami (ventral hypothalamus) (V13), including a few labeled cells per frontal section in the area of the ventral hypothalamus adjacent to the ventromedial tip of the infundibular recess [46].

AVT ISH-labeled cells were not found in either species in the *rostral medial mesencephalon* (V15). This area was found to contain AVT-immunoreactive cells in the earlier study of *T. granulosa* [46].

In both *P. shermani* and *T. granulosa*, AVT ISH-labeled cells were found near the midline of the *tectum mesencephali* (optic tectum). The intensity of labeling was typically light and limited to one to three cells per frontal section. AVT ISH-labeled cells were found in most individuals of *T. granulosa*, but only one individual *P. shermani*. These observations are unique in that these AVT-labeled cells were not identified previously with ICC.

Just rostral to the cerebellum, both species contained AVT ISH-labeled cells in the *nucleus visceralis superior-nucleus isthmi* region (V16) including the *nucleus posterior tecti*. However, in contrast to ICC findings, neither species had AVT ISH-labeled cells in the *nucleus cerebelli* (cerebellum) (V17) or, in the case of *P. shermani*, in the *inferior colliculus* (nucleus posterior tecti) (V18).

In the hindbrain, AVT ISH-labeled cells were found to be common in most *T. granulosa*, but only one individual of *P. shermani.* These AVT ISH-labeled cells were not described in previous studies. In *T. granulosa*, the AVT ISH-labeled cells in the hindbrain occurred at a level caudal to the trigeminal nerve and interpenduncular nucleus, in an area lateral to the raphe nucleus, and ventromedial to the area acousticolateralis and medial to the solitary tract. AVT labeling also occurred within the cell layer of the *stratum griseum* [32] just ventral of the fourth ventricle, and at this level, appeared to occur in the area of the *eminentia trigemini*. AVT ISH-labeled cells extended caudally through the levels of the *radix lateralis facialis*. Finally, in *P. shermani*, one individual (different from the one previously mentioned) was found to have an AVT ISH-labeled cell in an area just rostral of the spinal cord in the *stratum griseum* [35]; however, the precise level and region of this labeling were difficult determine due to tissue folding, but were estimated to occur between the level of the *IX root* and the level of the *lower vagus region* [35]. Because this labeling was found in only one individual, and due to its regional ambiguity, it was not designated as a discrete population.

3.3. Neuroanatomical distribution of MST ISH-labeled cells in P. shermani and T. granulosa

In contrast to the widespread distribution of AVT labeling, MST ISH-labeled cells were found to be restricted to the anterior hypothalamic/preoptic area of the caudal telencephalon and rostral diencephalon. In *P. shermani* and *T. granulosa*, MST ISH-labeled cells were found in the anterior preoptic area, with labeled cells occurring just caudal to the level of the bed nucleus of the stria terminalis. At this level, MST ISH-labeled cells were restricted to the dorsal portion of the anterior preoptic area.

At a more caudal level, MST ISH-labeled cells occurred in the anterior (ventral) preoptic area and extended dorsally into the posterior preoptic area. The large number of labeled cells in the posterior preoptic area formed a continuum with the labeled cells in the magnocellular preoptic area (Figs. 1B and 2B). In one individual *T. granulosa*, the MST ISH labeling in the posterior and magnocellular areas had the appearance of long, thin extensions emanating from the soma, indicating that perhaps MST mRNA had been translocated into the axons (Fig. 1B). In general, MST ISH-labeled cells in the anterior, posterior, and magnocellular preoptic areas were localized in more lateral positions, farther from the third ventricle, than were AVT containing cells. However, in some individuals of both species, MST ISH labeling occurred in more medial locations that overlap with AVT labeling. The MST ISH-labeling in the posterior preoptic area was limited rostrocaudally, usually disappearing caudally at approximately the level of the rostralmost dorsal habenula. In contrast, MST ISH-labeled cells of the dorsalmost magnocellular preoptic area persisted caudally, usually to just rostral of the level of the ventral hypothalamus.

Finally, MST ISH-labeled cells were found in the ventral thalamus of both species. The MST ISH labeling in the ventral thalamus was typically observed in its ventralmost region as part of an extension of a large population of MST ISH-labeled cells from the magnocellular preoptic area. However, some individuals of both species also possessed the MST ISH labeling in cells of the ventral thalamus that were distinct from the magnocellular population. These discrete MST ISH-labeled cells in the ventral thalamus typically were located centrally and usually had less intense labeling than the MST ISH-labeled cells extending into the ventral thalamus from the magnocellular preoptic area.

4. Discussion

4.1. AVT mRNA signal in the brains of P. shermani and T. granulosa

The AVT ISH-labeled cells in the brains from both *P. shermani* and *T. granulosa* had a widespread distribution, including clusters and scattered cells labeled in many various telencephalic and diencephalic regions. This widespread distribution of AVT ISH-labeled cells confirms that *T. granulosa* has a well-developed vasotocinergic system, as had been suggested by previous ICC studies [46,51]. Moreover, the finding that *P. shermani* closely matches *T. granulosa* in terms of the neuroanatomical distribution of AVT ISH-labeled-cells indicates that urodele amphibians synthesize AVT in many more extra-hypothalamic brain loci than other vertebrate taxa.

The current study also found AVT ISH-labeled cells in three brain areas where AVT had not been reported previously in an amphibian. Namely, AVT ISH-labeled cells occurred in the lateral pallium of *P. shermani*, the lateral septum of *T. granulosa*, and the optic tectum of both salamanders. Until now, AVT in the lateral pallium, lateral septum, and tectum of the amphibian brain was restricted to immunoreactive fibers [23,24,46], not AVT containing cell bodies. In mammals, AVP-containing cell bodies have been reported to occur in the lateral septum [62,65,66].

To organize the AVT system in *T. granulosa*, Lowry et al. [46] grouped AVT-labeled cells into nineteen defined cell populations (V1–V19). Many of these populations of AVT-immunoreactive cells in the brain of *T. granulosa* are not confined within established neuroanatomical boundaries [46]. Similarly, populations of AVT ISH-labeled cells in the current study were anatomically consistent with that earlier ICC study and frequently crossed defined neuroanatomical boundaries, generally matching the descriptions by Lowry et al. [46]. That study by Lowry et al. also included preliminary results from ISH studies that used AVT oligonucleotide probes (42 and 48 mers based on mammalian AVP sequence data). Those oligonucleotide probes labeled cells in six of the nineteen defined AVT-immunoreactive populations (V1, V2, V7, V8, V9, and V10). The current study used species-specific and gene-specific cRNA probes and labeled cells in brain areas that better matched the results from the previous ICC study (Table 1). In addition to labeling those populations previously identified with oligonucleotide probes, the cRNA probes in this study labeled populations V3–V6, and V11 in both species as well as V17 in *P. shermani* only. Furthermore, the cRNA probes used in this study labeled an additional AVT population in the optic tectum of both species. The presence of AVT cells in the tectum of *T. granulosa* was also observed using a digoxigenin (DIG)-labeled cRNA probe as well (data not shown). Finally, two more regions, the lateral pallium (*P. shermani*) and lateral septum (*T. granulosa*), were found to contain AVT ISH-labeled cells, indicating that there might be twenty-three populations of AVT cells in the urodele brain (Fig. 3). These different AVT populations, based on earlier research in *T. granulosa*, appear to be site-specifically regulated in a seasonal manner [52].

Table 1
Cell distribution of AVT and MST in the central nervous system of *T. granulosa* and *P. shermani*

Cell group	Immunocytochemistry[a]	In situ hybridization				
	AVP-ab	Oligo probes[a]	cRNA probe			
	T. granulosa AVT-like	*T. granulosa* AVT	*T. granulosa* AVT	MST	*P. shermani* AVT	MST
V1 Dorsal pallium-nucleus olfactorius anterior pars dorsalis continuum	•	•	•		•	
V2 Medial pallium	•	•	•		•	
Lateral pallium[b]					•	
V3 Caudal septum-medial basal forebrain continuum	•		•		•	
Lateral septum[c]			•			
V4 Bed nucleus of the stria terminalis	•		•		•	
V5 Nucleus amygdalae	•		•		•	
V6 Bed nucleus of the decussation of the fasciculus lateralis telencephali	•		•		•	
V7 Anterior preoptic area	•	•	•	♦	•	♦
V8 Pars ventralis thalami	•	•	•	♦	•	♦
V9 Magnocellular preoptic area	•	•	•	♦	•	♦
V10 Posterior preoptic area	•	•	•	♦	•	♦
V11 Ventral preoptic area	•		•	♦	•	♦
V12 Pars dorsalis hypothalami	•					
V13 Posterior lobe of the pars ventralis hypothalami	•		•			
V14 Primordial mammillary region	•					
V15 Rostral ventromedial mesencephalon	•					
V16 Nucleus visceralis superior-nucleus isthmi region	•		•		•	
Tectum mesencephali[c]			•		•	
V17 Nucleus cerebelli	•					
V18 Inferior colliculus	•		•			
V19 Lateral auricle-area acousticolateralis continuum	•					
Rostral medulla-eminentia trigemini[c]			•		•	

The distribution of AVT-immunoreactive cell bodies and AVT in situ hybridization signals by using either degenerate oligonucleotide probes (*T. granulosa*) or gene-specific cRNA probes *(T. granulosa* and *P. shermani*) is indicated with dots (•). The distribution of MST in *T. granulosa* and *P. shermani* is indicated with diamonds (♦).

[a] Lowry et al. [46].

[b] Population previously unidentified in vertebrates.

[c] Population previously unidentified in *T. granulosa*.

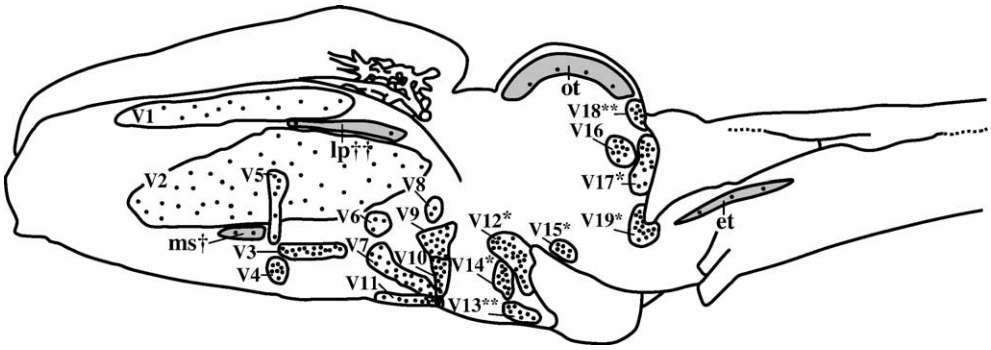

Fig. 3. Diagram of an adult *T. granulosa* brain illustrating 19 previously identified populations of AVT-immunoreactive cell bodies [46], with the addition of new populations of AVT ISH-labeled cells from both *T. granulosa* and *P. shermani* (original diagram from Moore and Lowry [51] has been modified). Black dots depict AVT-immunoreactive or ISH-labeled cells and their density, and the lines around the dots indicate approximate neuroanatomical boundaries for each group of AVT cell bodies and/or AVT ISH-labeled cells. The AVT-immunoreactive labeled cell populations of Lowry et al. [46] are labeled V1 through V19. Regions of AVT ISH-labeled cell populations not previously identified with ICC are shaded in gray and labeled with an abbreviation of the region (ms = medial septum, lp = lateral pallium, ot = optic tectum, and et = eminentia trigemini). A single asterisk (*) indicates an AVT-immunoreactive population that did not have AVT ISH-labeled cells in either species. Two asterisks (**) indicate an AVT-immunoreactive cell population that was observed with AVT ISH-labeled cells in just *T. granulosa*. A single dagger (†) indicates only AVT ISH labeling in just *T. granulosa* and two daggers (††) indicate only AVT ISH labeling in just *P. shermani*.

Agreement between the current ISH study and the previous ICC study was high, but not total. Populations of AVT-ir immunoreactivity in the brain of *T. granulosa* that remained unlabeled in this study were the dorsal hypothalamus (V12), the primordial mammillary region (V14), the rostral ventromedial mesencephalon (V15), and the area acousticolateralis (V19). The disparity between the ICC and ISH studies most likely reflects differences in sensitivity or lower abundance AVT mRNA, but it may also be due to the presence of splice-variants or multiple copies of the AVT-coding genes [46], as seen in teleosts [38,53]. There is currently no evidence for the latter explanation in amphibians. Our ISH protocol was optimized with high stringency conditions to reduce background noise.

The comparative distribution of AVT cell groups in the amphibian central nervous system is varied among (at least five) different genera, which includes *Taricha* [60]. The observed differences in AVT-labeled cells between *T. granulosa* and *P. shermani* are not unusual. Species differences in AVT or AVP cell distribution occur in reptiles [56]. Other observed species differences in AVT cell groups reported in reptiles and birds, and AVP cell groups in mammals, have been limited to relative AVT/AVP cell numbers in a given region rather than their presence or absence [8,13,61,67]. The inter-specific differences in the neuroanatomical localization of AVT ISH-labeled cells may reflect species specificity in neuronal pathways modulated by the AVT system in each of these urodele amphibians.

In addition to apparent inter-specific differences in AVT cell distribution, intra-specific differences were also observed, particularly in *P. shermani*, where not all individuals were observed with AVT ISH-labeled cells in the lateral pallium, tectum, and hindbrain. In *T. granulosa*, like *P. shermani*, not every individual labeled for the AVT mRNA signal in the tectum. Previous studies in our lab using radioimmunoassay show that AVT levels in the optic tectum of *T. granulosa* males change seasonally [69]. The current study was not designed to identify seasonal or sexual differences in AVT because the previous ICC with *T. granulosa* revealed that there are pronounced seasonal and sexual differences in AVT labeling [52]. Given those earlier findings, it seems reasonable that some of the observed intra-specific differences in AVT ISH labeling reflect differences in the physiological state of individual animals. In the rainbow trout (*Oncorhyncus mykiss*), stress (by acute confinement) influences regional AVT expression [21], while in the blennid fish (*Salaria pavo*), expression levels of AVT mRNA (on a per cell basis) are correlated with mating morphotype [30]. AVT gene expression and peptide secretion are affected by various factors including stage of metamorphosis [16,18,48], breeding season [27], hydromineral balance [69], environmental conditions [44], reproductive state [56], and the sex of the animal [16,17,30,31,52].

4.2. MST mRNA signal in the brains of P. shermani and T. granulosa

The current study is the first to describe the neuroanatomical distribution of MST ISH-labeled cells in an amphibian using gene-specific cRNA probes. Unlike AVT, MST ISH-labeled cells in both *P. shermani* and *T. granulosa* were limited to cells in the very caudal telencephalon, anterior hypothalamic preoptic areas, and only extended caudally to the level of the chiasmal ridge and habenular nuclei. This MST mRNA cell distribution was highly conserved in the brains of *P. shermani* and *T. granulosa* (see Table 1).

The most striking pattern regarding MST cells in the vertebrate central nervous system is its highly conserved distribution. The distribution of MST, or its orthologs, isotocin (IST) or OXY, in vertebrates is rarely found beyond regions of the caudal telencephalon and anterior diencephalon [9,11,27,57,64,68]. Exceptions are the reptilian rostral

hypothalamus [64], the avian ventral hypothalamus and medial septum [57], and mammalian lateral hypothalamus [68]. The distribution of MST ISH-labeled cells in *P. shermani* and *T. granulosa* showed no exceptions, with MST mRNA containing cells found only in regions of the preoptic area and ventral thalamus. Though this agrees with the pattern of MST-immunoreactive cell group distributions of other amphibians [60], exceptions in the amphibian have been shown in the bed nucleus of the stria terminalis of anurans [17,23], and the hypothalamus and tegmentum of caecilians (*Typhlonectes compressicauda* and *Typhlonectes natans*) [25,36]. The use of an MST oligonucleotide probe has shown specific MST cells in the medial pallium of *T. granulosa* [46]. The cRNA probe used in this study did not identify these cells. Whether this discrepancy reflects the differential regulation of the MST preprohormone in the brain of *T. granulosa*, probe specificity, or a difference in technique sensitivity is unknown. The different in situ hybridization techniques for oligonucleotide probes as opposed to cRNA probes may account for the incongruent results, as stringencies may differ. However, the higher specificity imparted by gene-specific cRNA probes, which failed to identify pallial MST mRNA, may indicate that detection of MST in the medial pallium depends on the physiological and/or behavioral state of the animal. Despite an unclear function for MST in non-mammalian vertebrates, its conservation from lungfishes to birds, excluding most fish, suggests its functions are conserved [4]. If the observed labeling represents MST differential regulation, it suggests that a modulatory role exists for MST in the amphibian central nervous system. Apart from the peripheral, physiological role of MST in parturition in marsupial mammals and its possible involvement in the regulation of water and salt transport in amphibians [5,10,43,59], no clear behavioral or neuromodulatory function has yet been ascribed to this peptide. Recent co-localization of MST immunoreactivity with that of opsin in the preoptic area has implicated MST in photoreception in *Xenopus laevis* [6]. Of interest, an individual of *T. granulosa* in this study exhibited ISH labeling in the posterior preoptic area, where not only cell bodies were labeled, but also axons extending from the cells exhibited high levels of expression as well, suggesting translocation of the gene. If this indicates MST mRNA translocation, it would further suggest that a possible neuromodulatory role exists for MST, which currently remains an enigma in this regard.

4.3. Conclusion

In conclusion, AVT ISH-labeled cells were widely distributed in the brains of *T. granulosa* and *P. shermani*, whereas MST ISH-labeled cells were limited to a very narrow range of distribution. The overall pattern for AVT distribution matches patterns seen in other vertebrate classes, but both species of salamander were found to possess the most extensive AVT cell populations of any vertebrate described thus far. The current study provides further evidence that the AVT system in urodele amphibians has an unusually extensive neuroanatomical distribution. In contrast, the localization of MST-expressing cells in urodeles suggests that its distribution has been highly conserved throughout evolution.

Acknowledgments

We thank Stevan Arnold, Sam Bradford, Emma Coddington, Jonathan Feder, Pam Feldhoff, Rick Feldhoff, Renee Fox, Lynne Houck, Catherine Palmer, Melody Rudenko, Richard Watts, Mike Westphal, and Garret Woodman for the collection of animals and/or tissue extraction. We also thank TJ White and Tom Zoeller for technical assistance and Barbara Taylor for digital imaging. This study was supported by the National Science Foundation (IBN-0110666).

References

[1] R. Acher, Neurohypophysial peptide systems: processing machinery, hydroosmotic regulation, adaptation and evolution, Regul. Pept. 45 (1993) 1–13.
[2] R. Acher, Molecular evolution of fish neurohypophysial hormones: neutral and selective evolutionary mechanisms, Gen. Comp. Endocrinol. 102 (1996) 157–172.
[3] R. Acher, J. Chauvet, Structure, processing and evolution of the neurohypophysial hormone-neurophysin precursors, Biochimie 70 (1988) 1197–1207.
[4] R. Acher, J. Chauvet, M.T. Chauvet, Man and the chimaera. Selective versus neutral oxytocin evolution, Adv. Exp. Med. Biol. 395 (1995) 615–627.
[5] A. Akhundova, E. Getmanova, V. Gorbulev, E. Carnazzi, P. Eggena, F. Fahrenholz, Cloning and functional characterization of the amphibian mesotocin receptor, a member of the oxytocin/vasopressin receptor superfamily, Eur. J. Biochem. 237 (1996) 759–767.
[6] M. Alvarez-Viejo, R. Cernuda-Cernuda, W.J. DeGrip, C. Alvarez-Lopez, J.M. Garcia-Fernandez, Co-localization of mesotocin and opsin immunoreactivity in the hypothalamic preoptic nucleus of *Xenopus laevis*, Brain Res. 969 (2003) 36–43.
[7] A. Argiolas, G.L. Gessa, Central functions of oxytocin, Neurosci. Biobehav. Rev. 15 (1991) 217–231.
[8] N. Aste, E. Muhlbauer, R. Grossmann, Distribution of AVT gene expressing neurons in the prosencephalon of Japanese quail and chicken, Cell Tissue Res. 286 (1996) 365–373.
[9] S.W. Barth, R.A. Bathgate, A. Mess, L.J. Parry, R. Ivell, R. Grossmann, Mesotocin gene expression in the diencephalon of domestic fowl: cloning and sequencing of the MT cDNA and distribution of MT gene expressing neurons in the chicken hypothalamus, J. Neuroendocrinol. 9 (1997) 777–787.
[10] R.A. Bathgate, L.J. Parry, T.P. Fletcher, G. Shaw, M.B. Renfree, R.T. Gemmell, C. Sernia, Comparative aspects of oxytocin-like hormones in marsupials, Adv. Exp. Med. Biol. 395 (1995) 639–655.
[11] T.F. Batten, M.L. Cambre, L. Moons, F. Vandesande, Comparative distribution of neuropeptide-immunoreactive systems in the brain of the green molly, *Poecilia latipinna*, J. Comp. Neurol. 302 (1990) 893–919.
[12] M. Bennis, A.M. Tramu, J. Reperant, Vasopressin- and oxytocin-like systems in the chameleon brain, J. Hirnforsch. 36 (1995) 445–450.
[13] J.K. Bester-Meredith, L.J. Young, C.A. Marler, Species differences in

paternal behavior and aggression in peromyscus and their associations with vasopressin immunoreactivity and receptors, Horm. Behav. 36 (1999) 25–38.
[14] H.C. Birnboim, J. Doly, A rapid alkaline extraction procedure for screening recombinant plasmid DNA, Nucleic Acids Res. 7 (1979) 1513–1523.
[15] N. Bons, The topography of mesotocin and vasotocin systems in the brain of the domestic mallard and Japanese quail: immunocytochemical identification, Cell Tissue Res. 213 (1980) 37–51.
[16] S.K. Boyd, Arginine vasotocin facilitation of advertisement calling and call phonotaxis in bullfrogs, Horm. Behav. 28 (1994) 232–240.
[17] S.K. Boyd, C.J. Tyler, G.J. De Vries, Sexual dimorphism in the vasotocin system of the bullfrog (*Rana catesbeiana*), J. Comp. Neurol. 325 (1992) 313–325.
[18] J.A. Carr, D.O. Norris, Immunohistochemical localization of corticotropin-releasing factor- and arginine vasotocin-like immunoreactivities in the brain and pituitary of the American bullfrog (*Rana catesbeiana*) during development and metamorphosis, Gen. Comp. Endocrinol. 78 (1990) 180–188.
[19] M.M. Caverson, J. Ciriello, F.R. Calaresu, T.L. Krukoff, Distribution and morphology of vasopressin-, neurophysin II-, and oxytocin-immunoreactive cell bodies in the forebrain of the cat, J. Comp. Neurol. 259 (1987) 211–236.
[20] V.J. Choy, W.B. Watkins, HPLC separation of vasopressin-like hormones in chicken neurohypophysial extracts, Neuropeptides 8 (1986) 183–191.
[21] B.J. Gilchriest, D.R. Tipping, L. Hake, A. Levy, B.I. Baker, The effects of acute and chronic stresses on vasotocin gene transcripts in the brain of the rainbow trout (*Oncorhynchus mykiss*), J. Neuroendocrinol. 12 (2000) 795–801.
[22] G. Gimpl, F. Fahrenholz, The oxytocin receptor system: structure, function, and regulation, Physiol. Rev. 81 (2001) 629–683.
[23] A. Gonzalez, W.J. Smeets, Comparative analysis of the vasotocinergic and mesotocinergic cells and fibers in the brain of two amphibians, the anuran *Rana ridibunda* and the urodele *Pleurodeles waltlii*, J. Comp. Neurol. 315 (1992) 53–73.
[24] A. Gonzalez, W.J. Smeets, Distribution of vasotocin- and mesotocin-like immunoreactivities in the brain of the South African clawed frog *Xenopus laevis*, J. Chem. Neuroanat. 5 (1992) 465–479.
[25] A. Gonzalez, W.J. Smeets, Distribution of vasotocin- and mesotocin-like immunoreactivities in the brain of *Typhlonectes compressicauda* (Amphibia, gymnophiona): further assessment of primitive and derived traits of amphibian neuropeptidergic systems, Cell Tissue Res. 287 (1997) 305–314.
[26] J.L. Goodson, A.H. Bass, Social behavior functions and related anatomical characteristics of vasotocin/vasopressin systems in vertebrates, Brain Res. Brain Res. Rev. 35 (2001) 246–265.
[27] J.L. Goodson, A.K. Evans, A.H. Bass, Putative isotocin distributions in sonic fish: relation to vasotocin and vocal-acoustic circuitry, J. Comp. Neurol. 462 (2003) 1–14.
[28] N. Goossens, K. Dierickx, F. Vandesande, Immunocytochemical study of the neurohypophysial hormone producing system of the lungfish, *Protopterus aethiopicus*, Cell Tissue Res. 190 (1978) 69–77.
[29] N. Goossens, K. Dierickx, F. Vandesande, Immunocytochemical localization of vasotocin and mesotocin in the hypothalamus of lacertilian reptiles, Cell Tissue Res. 200 (1979) 223–227.
[30] M.S. Grober, A.A. George, K.K. Watkins, L.A. Carneiro, R.F. Oliveira, Forebrain AVT and courtship in a fish with male alternative reproductive tactics, Brain Res. Bull. 57 (2002) 423–425.
[31] R. Grossmann, A. Jurkevich, A. Kohler, Sex dimorphism in the avian arginine vasotocin system with special emphasis to the bed nucleus of the stria terminalis, Comp. Biochem. Physiol., Part A: Mol. Integr. Physiol. 131 (2002) 833–837.
[32] C.J. Herrick, The medulla oblongata of larval Amblystoma, J. Comp. Neurol. 24 (1914) 343–427.
[33] C.J. Herrick, The amphibian forebrain: III. The optic tracts and centers of *Amblystoma* and the frog, J. Comp. Neurol. 39 (1925) 433–489.
[34] C.J. Herrick, The amphibian forebrain: IV. The cerebral hemispheres of *Amblystoma*, J. Comp. Neurol. 43 (1927) 231–325.
[35] C.J. Herrick, The Brain of the Tiger Salamander, *Ambyostoma tigrinum*, The University of Chicago Press, Chicago and London, 1948.
[36] C. Hilscher-Conklin, J.M. Conlon, S.K. Boyd, Identification and localization of neurohypophysial peptides in the brain of a caecilian amphibian, *Typhlonectes natans* (Amphibia: Gymnophiona), J. Comp. Neurol. 394 (1998) 139–151.
[37] L.D. Houck, L.N. Reagan, Male courtship pheromones increase female receptivity in a plethodontid salamander, Horm. Behav. 39 (1990) 729–734.
[38] S. Hyodo, Y. Kato, M. Ono, A. Urano, Cloning and sequence analyses of cDNAs encoding vasotocin and isotocin precursors of chum salmon, *Oncorhynchus keta*: evolutionary relationships of neurohypophysial hormone precursors, J. Comp. Physiol., B 160 (1991) 601–608.
[39] S. Hyodo, S. Ishii, J.M. Joss, Australian lungfish neurohypophysial hormone genes encode vasotocin and[Phe2]mesotocin precursors homologous to tetrapod-type precursors, Proc. Natl. Acad. Sci. U. S. A. 94 (1997) 13339–13344.
[40] T.R. Insel, L. Young, Z. Wang, Central oxytocin and reproductive behaviours, Rev. Reprod. 2 (1997) 28–37.
[41] R. Ivell, T. Kimura, D. Muller, K. Augustin, N. Abend, R. Bathgate, R. Telgmann, M. Balvers, G. Tillmann, A.R. Fuchs, The structure and regulation of the oxytocin receptor, Exp. Physiol. 86 (2001) 289–296.
[42] Y. Jokura, A. Urano, Extrahypothalamic projection of immunoreactive vasotocin fibers in the brain of the toad, *Bufo japonicus*, Zool. Sci. 4 (1987) 675–681.
[43] S. Kohno, Y. Kamishima, T. Iguchi, Molecular cloning of an anuran V(2) type[Arg(8)] vasotocin receptor and mesotocin receptor: functional characterization and tissue expression in the Japanese tree frog (*Hyla japonica*), Gen. Comp. Endocrinol. 132 (2003) 485–498.
[44] S.C. Lema, G.A. Nevitt, Variation in vasotocin immunoreactivity in the brain of recently isolated populations of a death valley pupfish, *Cyprinodon nevadensis*, Gen. Comp. Endocrinol. 135 (2004) 300–309.
[45] P. Licht, B.T. Pickering, H. Papkoff, A. Pearson, A. Bona-Gallo, Presence of a neurophysin-like precursor in the green turtle (*Chelonia mydas*), J. Endocrinol. 103 (1984) 97–106.
[46] C.A. Lowry, C.F. Richardson, T.R. Zoeller, L.J. Miller, L.E. Muske, F.L. Moore, Neuroanatomical distribution of vasotocin in a urodele amphibian (*Taricha granulosa*) revealed by immunohistochemical and in situ hybridization techniques, J. Comp. Neurol. 385 (1997) 43–70.
[47] T. Maniatis, E.F. Fritsch, J. Sambrook, Isolation of bacteriophage γ and plasmid DNA, Molecular Cloning: A Laboratory Manual, Cold Spring Harbor Laboratory, Cold Spring Harbor, NY, 1982, pp. 75–96.
[48] W.B. Mathieson, Development of arginine vasotocin innervation in two species of anuran amphibian: *Rana catesbeiana* and *Rana sylvatica*, Histochem. Cell Biol. 105 (1996) 305–318.
[49] P. Micevych, R. Elde, Relationship between enkephalinergic neurons and the vasopressin-oxytocin neuroendocrine system of the cat: an immunohistochemical study, J. Comp. Neurol. 190 (1980) 135–146.
[50] F.L. Moore, Evolutionary precedents for behavioral actions of oxytocin and vasopressin, Ann. N. Y. Acad. Sci. 652 (1992) 156–165.
[51] F.L. Moore, C.A. Lowry, Comparative neuroanatomy of vasotocin and vasopressin in amphibians and other vertebrates, Comp. Biochem. Physiol., Part C: Pharmacol. Toxicol. Endocrinol. 119 (1998) 251–260.
[52] F.L. Moore, C. Richardson, C.A. Lowry, Sexual dimorphism in numbers of vasotocin-immunoreactive neurons in brain areas associated with reproductive behaviors in the roughskin newt, Gen. Comp. Endocrinol. 117 (2000) 281–298.
[53] S.D. Morley, C. Schonrock, J. Heierhorst, J. Figueroa, K. Lederis, D. Richter, Vasotocin genes of the teleost fish *Catostomus commersoni*: gene structure, exon–intron boundary, and hormone precursor organization, Biochemistry 29 (1990) 2506–2511.

[54] H. Nojiri, I. Ishida, E. Miyashita, M. Sato, A. Urano, T. Deguchi, Cloning and sequence analysis of cDNAs for neurohypophysial hormones vasotocin and mesotocin for the hypothalamus of toad, *Bufo japonicus*, Proc. Natl. Acad. Sci. U. S. A. 84 (1987) 3043–3046.
[55] R.G. Northcutt, E. Kicliter, Organization of the amphibian telencephalon, in: S.O.E. Ebbesson (Ed.), Comparative Neurology of the Telencephalon, Plenum Press, New York, 1980, pp. 203–255.
[56] C.R. Propper, R.E. Jones, K.H. Lopez, Distribution of arginine vasotocin in the brain of the lizard *Anolis carolinensis*, Cell Tissue Res. 267 (1992) 391–398.
[57] B. Robinzon, T.I. Koike, H.L. Neldon, S.L. Kinzler, Distribution of immunoreactive mesotocin and vasotocin in the brain and pituitary of chickens, Peptides 9 (1988) 829–833.
[58] J.D. Rose, F.L. Moore, Behavioral neuroendocrinology of vasotocin and vasopressin and the sensorimotor processing hypothesis, Front. Neuroendocrinol. 23 (2002) 317–341.
[59] G. Shaw, M.B. Renfree, Fetal control of parturition in marsupials, Reprod. Fertil. Dev. 13 (2001) 653–659.
[60] W.J. Smeets, A. Gonzalez, Vasotocin and mesotocin in the brains of amphibians: state of the art, Microsc. Res. Tech. 54 (2001) 125–136.
[61] W.J. Smeets, J.J. Sevensma, A.J. Jonker, Comparative analysis of vasotocin-like immunoreactivity in the brain of the turtle *Pseudemys scripta elegans* and the snake *Python regius*, Brain Behav. Evol. 35 (1990) 65–84.
[62] M.V. Sofroniew, Vasopressin- and neurophysin-immunoreactive neurons in the septal region, medial amygdala and locus coeruleus in colchicine-treated rats, Neuroscience 15 (1985) 347–358.
[63] M.V. Sofroniew, A. Weindl, I. Schinko, R. Wetzstein, The distribution of vasopressin-, oxytocin-, and neurophysin-producing neurons in the guinea pig brain: I. The classical hypothalamo-neurophypophyseal system, Cell Tissue Res. 196 (1979) 367–384.
[64] T. Thepen, P. Voorn, C.J. Stoll, A.A. Sluiter, C.W. Pool, A.H. Lohman, Mesotocin and vasotocin in the brain of the lizard *Gekko gecko*. An immunocytochemical study, Cell Tissue Res. 250 (1987) 649–656.
[65] F.J. van Eerdenburg, D.F. Swaab, F.W. van Leeuwen, Distribution of vasopressin and oxytocin cells and fibres in the hypothalamus of the domestic pig (*Sus scrofa*), J. Comp. Neurol. 318 (1992) 138–146.
[66] F. van Leeuwen, R. Caffe, Vasopressin-immunoreactive cell bodies in the bed nucleus of the stria terminalis of the rat, Cell Tissue Res. 228 (1983) 525–534.
[67] C. Viglietti-Panzica, Immunohistochemical study of the distribution of vasotocin reacting neurons in avian diencephalon, J. Hirnforsch. 27 (1986) 559–566.
[68] Z. Wang, L. Zhou, T.J. Hulihan, T.R. Insel, Immunoreactivity of central vasopressin and oxytocin pathways in microtine rodents: a quantitative comparative study, J. Comp. Neurol. 366 (1996) 726–737.
[69] R.T. Zoeller, F.L. Moore, Brain arginine vasotocin concentrations related to sexual behaviors and hydromineral balance in an amphibian, Horm. Behav. 22 (1988) 66–75.
[70] R.T. Zoeller, D.L. Fletcher, O. Butnariu, C.A. Lowry, F.L. Moore, N-ethylmaleimide (NEM) can significantly improve in situ hybridization results using 35S-labeled oligodeoxynucleotide or complementary RNA probes, J. Histochem. Cytochem. 45 (1997) 1035–1041.